SiliconPV 2024, 14th International Conference on Crystalline Silicon Photovoltaics

Silicon Material and Defect Engineering

https://doi.org/10.52825/siliconpv.v2i.1312

© Authors. This work is licensed under a Creative Commons Attribution 4.0 International License

Published: 09 Jan. 2025

Understanding Hydrogen Passivation Mechanism in *poly*-Si Passivating Contacts via Si_xN_y Composition: Insights From Effusion Studies

Suchismita Mitra[1], Dirk Steyn[2], William Nemeth[1], Sumit Agarwal[2], and Paul Stradins[1]

[1] National Renewable Energy Laboratory, USA

[2] Colorado School of Mines, USA

*Correspondence: Paul Stradins, pauls.stradins@nrel.gov

Abstract. Tunnel Oxide Passivated Contact (TOPCon) cell performance relies significantly on hydrogen for its passivation of defects. In this paper, we discuss the temperature dependent effusion of hydrogen from the silicon nitride (Si_xN_y) layers deposited on top of poly-Si/SiO_2 passivated contacts. Silicon content in Si_xN_y was varied by silane/ammonia flow ratio. FTIR shows significant N-H stretching & bending peaks for nitrogen-rich Si_xN_y layer compared to silicon-rich Si_xN_y layer, and less Si-H bonds compared to silicon-rich Si_xN_y. During effusion, the N-H bonds in N-rich Si_xN_y layer break to provide H_2, NH_3 and N_2, resulting in stoichiometry change. Negligible effusion of nitrogen occurs for Si-rich Si_xN_y layers. Next, we investigate the mechanism of hydrogen passivation on symmetrical i-*poly*-Si/SiO_2/c-Si/SiO_2/i-*poly*-Si structures with different hydrogenating layers namely Si-rich Si_xN_y, Al_2O_3 and a stack of Al_2O_3/Si_xN_y, and conclude that a thin 15 nm Al_2O_3 enables the best passivation. We also discuss the possibility of H diffusion in molecular H_2 form, most suitable for SiO_2 interface passivation, while the atomic hydrogen enables both passivation and de-passivation of interface dangling bonds.

Keywords: TOPCon Cells, Hydrogen Effusion, Defect Passivation, Silicon Nitride Layers, Aluminium Oxide Layers

1. Introduction

Traditionally, hydrogen-rich amorphous layers like amorphous silicon nitride (a-SiN_x:H) and amorphous silicon (a-Si:H), have been used for surface passivation in high efficiency c-Si solar cells. In Tunnel Oxide Passivated Contact (TOPCon) structures, an ultra-thin SiO_x layer (1-2 nm) is sandwiched between c-Si and *poly*-Si. A H-source layer such as Al_2O_3, Si_xN_y, or stack of Al_2O_3/Si_xN_y is deposited on *poly*-Si. When the device undergoes high temperature firing process during metallization, a significant amount of hydrogen is released from the hydrogenated film. While most of the hydrogen effuses into the ambient, some of the hydrogen travels inwards and passivates defects in *poly*-Si and at the SiO_x/c-Si interface [1]. A part of it can also diffuse into the bulk c-Si. Although hydrogen helps in passivation, excess hydrogen can also be responsible for poor performance of devices indicating the requirement of an optimized amount of hydrogen [2]. Simulations by Diggs et al. [3] show that excess hydrogen facilitates nucleation of Si-rich "pinholes" in SiO_x, which increases the concentration of dangling bonds, thereby increasing recombination. Interestingly, the simulations suggest that removal of hydrogen dissolves the "pinholes", thereby reversibly reducing recombination. Studies have also shown that there is a strong correlation between the bulk hydrogen concentration and Light elevated and Temperature Induced Degradation (LeTID), though the mechanism is not yet

understood [4]. The form in which hydrogen is released, i.e. atomic or molecular, can also affect passivation and hydrogen effusion. While molecular hydrogen only passivates defects at the SiO_2/Si interface (P_b+H_2 → P_bH+H), atomic hydrogen can lead to both passivation and abstraction (depassivation) (P_b+H^o → P_bH, P_bH+H^o → P_b+H_2), see Ref. [5]. Thus, it is necessary to understand the amount, transportation (molecular or atomic) and passivation mechanism by hydrogen in *poly*-Si/SiO_x/c-Si structures.

It has been observed that Si_xN_y:H contains a larger amount of hydrogen compared to Al_2O_3:H, but passivation is mediocre; while AlO_x:H leads to much better passivation with much less bonded H in the poly-Si. According to the hypothesis proposed by Truong et al. [6], hydrogen from the Si_xN_y:H film can passivate dangling bonds of the disordered Si phase more effectively than hydrogen from the Al_2O_3:H film owing to the different "types" of hydrogen emitted from the two different dielectric layers into the *poly*-Si films. In this work, we aim to establish the possible hydrogen bonding configurations, both in the overlaying dielectric stacks, and in the *poly*-Si itself, using H-effusion mass spectroscopy and FTIR spectroscopy. We also show that H-effusion proceeds very differently depending on composition of Si_xN_y. We present the H-effusion from *poly*-Si only by measuring H-effusion after chemically removing the dielectric layers.

2. Experimental details

The first set of samples was prepared by depositing Si_xN_y on both sides of n-CzSi by varying the SiH_4 flow (2 sccm and 8 sccm) during deposition in the PECVD chamber. The deposition conditions are given in Table 1.

Table 1. *Si_xN_y deposition parameters in PECVD*

Deposition Parameters	Set 1	Set 2
Heater Temperature (°C)	350	350
SiH_4 Flow (sccm)	8	2
NH_3 Flow (sccm)	24	24
Run Pressure (Torr)	0.45	0.45
Deposition Time (min)	6	9

The second set of samples was prepared similar to Truong's experiment [6], see Figure 1. In these samples, the *poly*-Si was hydrogenated by four different methods, forming gas annealing (FGA), Al_2O_3, Si_xN_y and a stack of Al_2O_3/Si_xN_y. Effusion measurements were done in presence of dielectric layers and also after removing them to see the amount of H_2 effusion from *poly*-Si. The 30 mm x 50 mm samples were prepared from <100> n-type Si Cz M4 wafers using a laser scriber. The surface was planarized using KOH ~30 mins @ 50°C until surface appears specular. After that, the samples were cleaned via RCA1, RCA2 and piranha. Subsequently, the wafers went for low-T thermal oxidation (LTO) at 550°C for 10 minutes in O_2 and N_2. The SiO_2 layer formed was 1.3 nm as measured by spectroscopic ellipsometry. This was followed by a deposition of intrinsic a-Si of 50 nm on both sides of the wafers which was then crystallized at 850°C for 30 min forming *poly*-Si. Intrinsic poly-Si was used here to reduce field effect passivation and emphasize chemical passivation of the SiO_2/Si interface. At this point the wafers were divided into three groups as shown in Figure 1. In the Group 1, after an HF dip, the samples were subjected to Al_2O_3:H deposition of 15 nm by 150 cycles on both sides using atomic layer deposition (ALD) followed by forming gas annealing (FGA) at 400°C and removal of the Al_2O_3:H layer using HF. Minority carrier lifetime, PL imaging, FTIR and effusion was done at this stage. The samples which were used for effusion measurement were not processed further as this measurement technique destroys the samples. Group 2 receives

Si_xN_y:H deposition and subsequent FGA at 400°C. A stack of Al_2O_3/Si_xN_y is deposited on the remaining samples from Group 3 followed by FGA at 400°C. After removing the dielectric layer using HF, minority carrier lifetime, PL imaging, FTIR and hydrogen effusion was measured again.

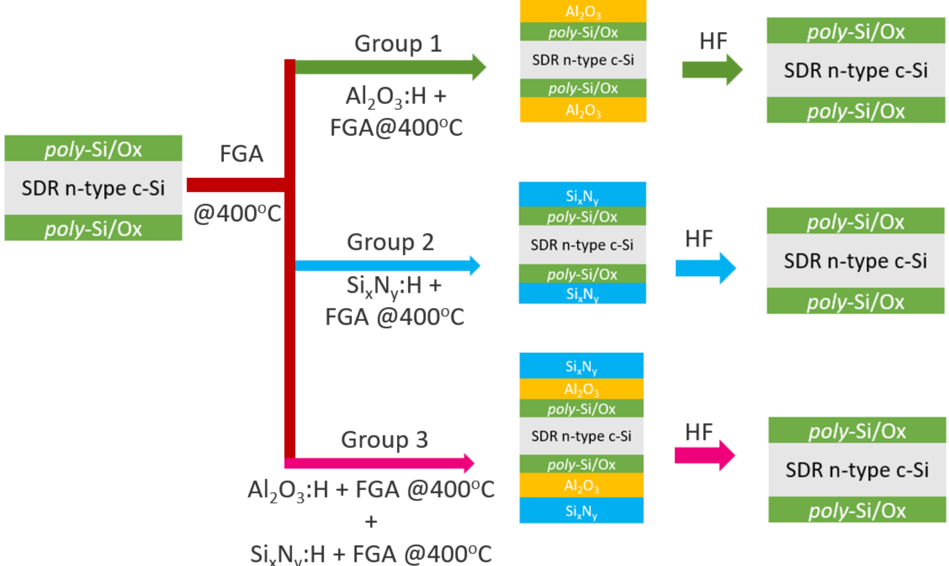

Figure 1. *Sample preparation for effusion studies*

3. Results and Discussions

3.1 H-bonding in two types of nitride

The refractive index for N-rich (SiH_4 flow=2 sccm) and Si-rich (SiH_4 flow =8 sccm) Si_xN_y layers is shown in Figure 2 and FTIR results of Si_xN_y/c-Si/ Si_xN_y samples are shown in Figure 3. While the solid line shows FTIR before effusion, the dotted line shows FTIR after effusion. Clearly, N-rich Si_xN_y layers with lower refractive index and high UV-transmittance have significant N-H bending and stretching bonds compared to Si-rich Si_xN_y layers. These N-H bonds are lost after effusion. On the other hand, Si-rich Si_xN_y layers have significant Si-H stretching bonds and significantly less N-H bonds, both lost after effusion of H.

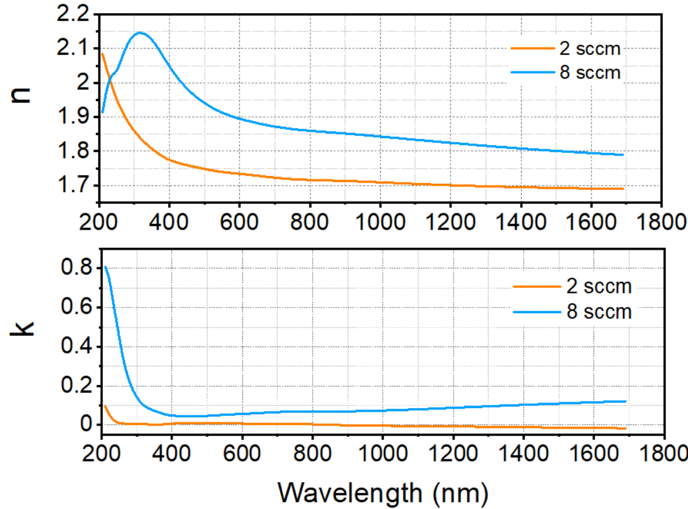

Figure 2. *Refractive index of N-rich (SiH_4 flow = 2 sccm) and Si-rich Si_xN_y layer (SiH_4 flow = 8 sccm)*

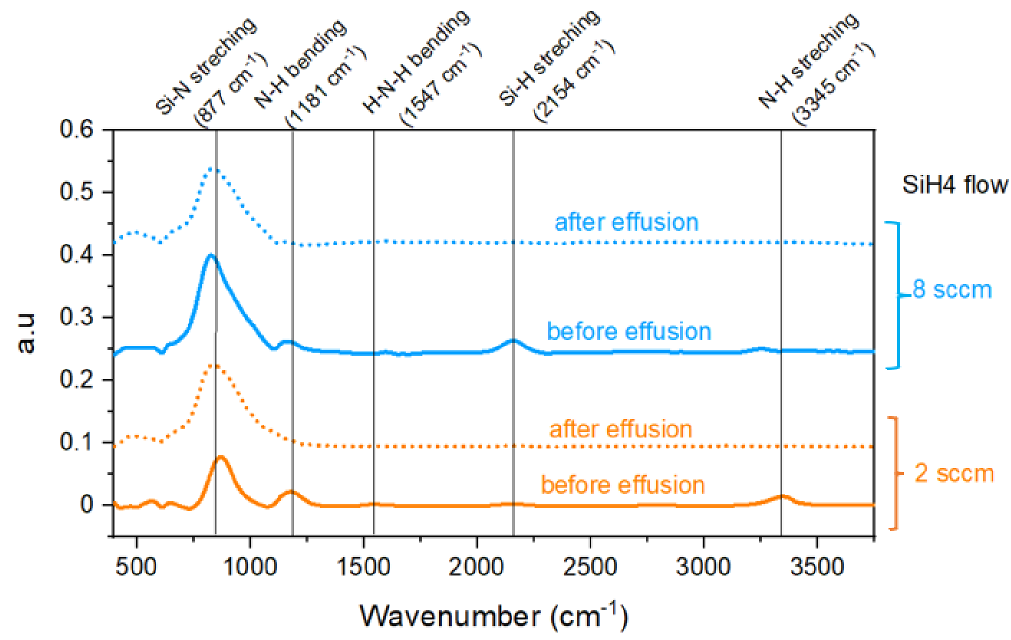

Figure 3. *FTIR of N-rich and Si-rich Si_xN_y layer before and after H effusion to 1000 °C.*

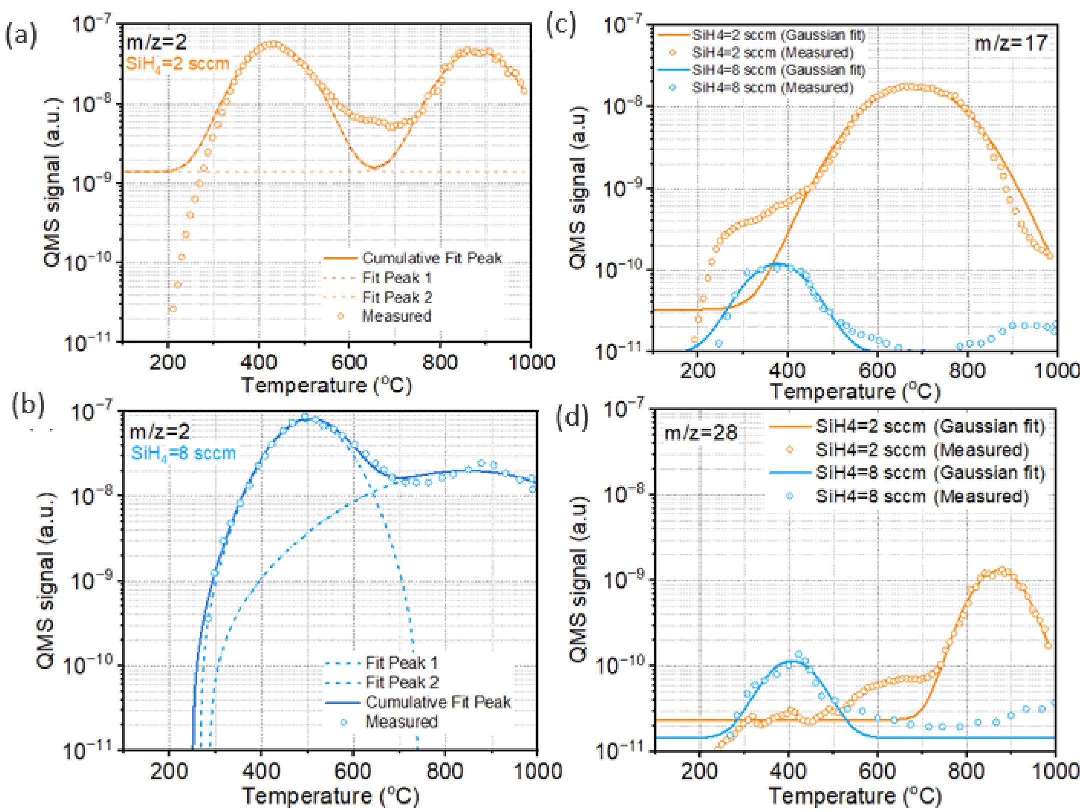

Figure 4. *Effusion profiles for (a) N-rich Si_xN_y, m/z=2 (b) Si-rich Si_xN_y, m/z=2; both layers (c) m/z=17 (d) m/z=28. Solid curves are Gaussian fits revealing deconvoluted effusion peaks.*

3.2 Effusion from symmetric Si_xN_y/c-Si/ Si_xN_y structures

Effusion results for symmetric Si_xN_y/c-Si/ Si_xN_y, as shown in Fig. 4, exhibit two distinct peaks for H_2 for N-rich Si_xN_y layers (437°C and 883°C) but only one main peak for Si-rich Si_xN_y layers at low temperature of 503°C. The peak temperatures of H_2 effusion may be due to the difference in strength of Si−H and N−H bonds. The weaker Si−H bonds break at a lower temperature compared to the stronger N−H bonds [4]. For N-rich Si_xN_y layers, nitrogen also effuses as NH_3 (m/z=17) and N_2 (m/z=28) at around 600 - 900 °C. In contrast, these species effuse in much

lesser amounts in Si-rich Si_xN_y layers. This indicates that the stoichiometry of Si_xN_y is changing during high temperature annealing of N-rich Si_xN_y layers.

Table 2. *Peak temperatures after Gaussian deconvolution of effusion curve*

SiH4 flow (sccm)	Mass/charge (m/z)	Peak I (°C)	Peak II (°C)
2	2	437	883
	17	-	680
	28	-	874
8	2	503	852
	17	-	-
	28	409	-

3.3 Effusion from symmetric hydrogenated i-*poly*-Si/SiO_x/c-Si structures

The m/z = 2 effusion profiles from symmetric i-*poly*-Si/SiO_x/c-Si structures with different H-source dielectric layers are shown in Figure 5, 6 and 7. These samples have undergone FGA at 400°C before the effusion measurement. Figure 5, the blue curve shows the effusion from *poly*-Si/SiOx/c-Si samples with Si_xN_y layer (8 sccm) present. It follows the same trend as symmetric Si_xN_y deposition on c-Si. When the Si_xN_y is removed by dipping in HF and effusion measurements are performed, it is found that that H_2 effusion from the *poly*-Si takes place at 400°C and the total amount of effused H_2 is reduced ~ 100x. Si-rich Si_xN_y has been chosen for this study as it is more stable during high temperature treatments compared to N-rich Si_xN_y. The iV_{oc} reduced from 655 mV from the presence of Si_xN_y to 620 mV when the layer was removed by dipping the sample in HF before the effusion measurement. This might be due to blisters in *poly*-Si which have led to formation of pinholes in the SiO_x layer leading to a reduction in passivation.

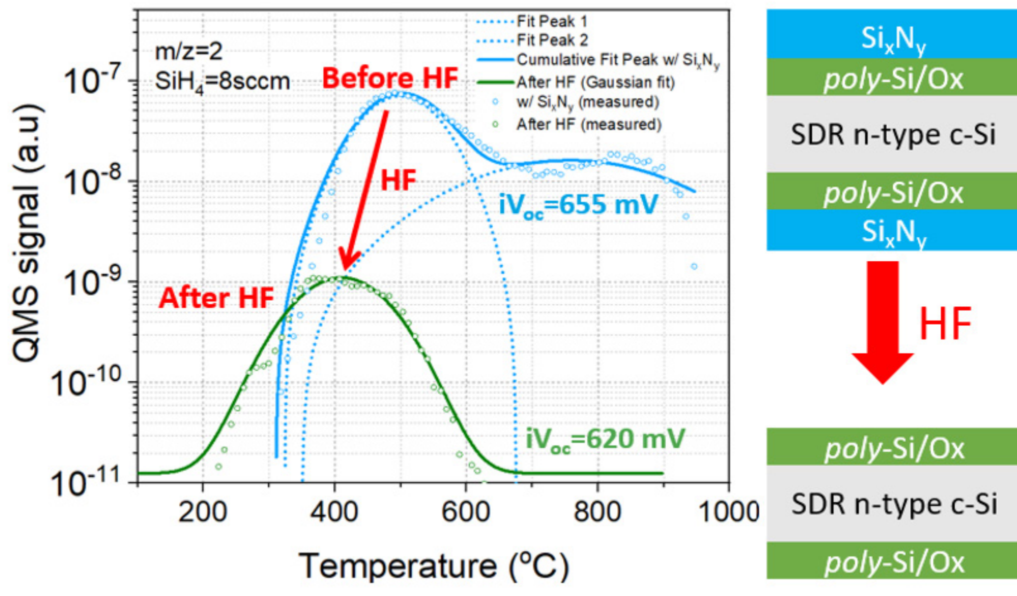

Figure 5. *Effusion profile for poly-Si samples with Si_xN_y passivation*

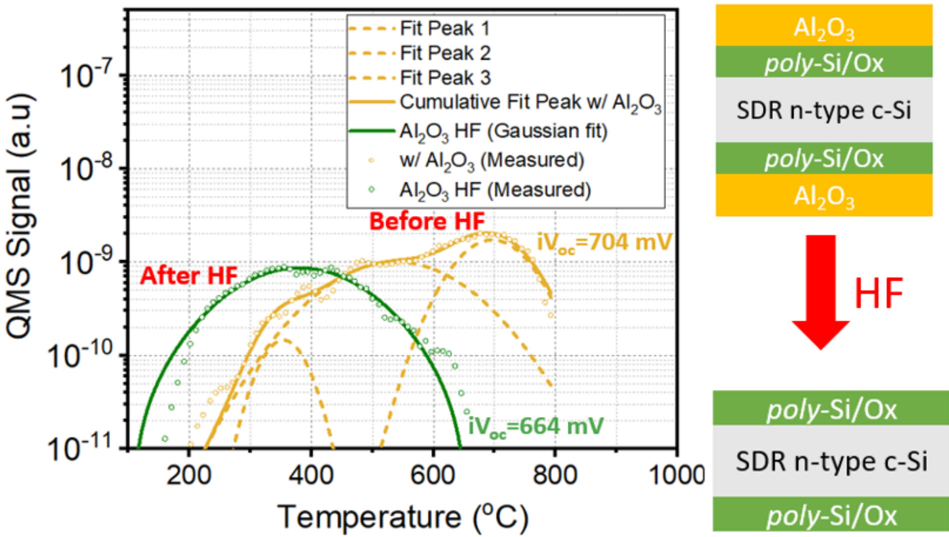

Figure 6. *Effusion profile for poly-Si samples with Al_2O_3 passivation*

In the case of Al_2O_3 in Figure 6, Gaussian deconvolution of the effusion profile shows there are three peaks, the highest being at 695°C. The amount of hydrogen effused is much lower than Si_xN_y as the [H] in alumina is ~ 4 at. % while ~ 30 at. % in SiN_x, and the alumina film is also thinner that the nitride (15 nm vs. 70 nm). Still, this lower amount of H leads to a better passivation with iV_{oc} =704 mV. Effusion at higher temperature and better passivation despite lower hydrogen indicates that the hydrogen released from Al_2O_3 might either be different from Si_xN_y (for example, predominantly H_2 diffusing towards the SiO_2 interface), or its amount is so much lower that the H-abstraction reaction from the P_{b0} interface defects (see above) is supressed. However, when the Al_2O_3 is removed by HF, the H-effusion from the poly-Si occurs at 400°C just like for the Si_xN_y sample. Furthermore, the effused H_2 amount is almost identical, even though the Al_2O_3 is thinner than the Si_xN_y layer.

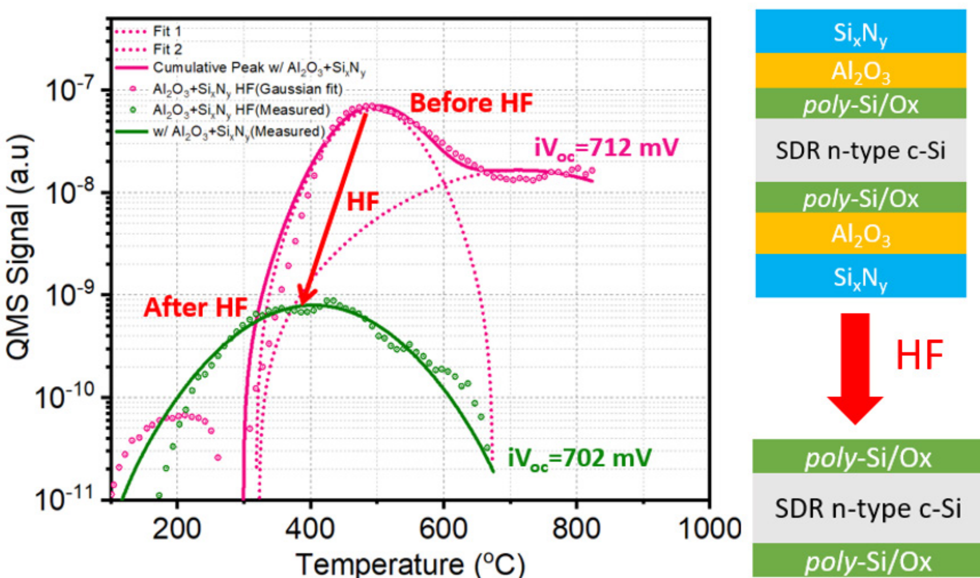

Figure 7. *Effusion profile for poly-Si samples with Al_2O_3/Si_xN_y passivation*

Figure 7 shows the H_2 effusion profile for an Al_2O_3/Si_xN_y stack. The effusion profile is similar to that of a single Si_xN_y layer, as the hydrogen effused from Si_xN_y layer dominates. But, it may be noted that the iV_{oc} in presence of Al_2O_3/Si_xN_y stack is 712 mV indicating the effect of passivation due to the presence of the Al_2O_3 layer, which likely acts as a barrier to excessive hydrogenation of the SiO_2 interface.

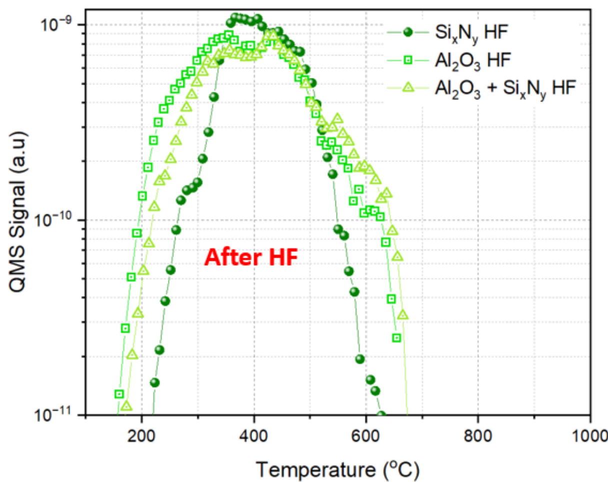

Figure 8. *H-effusion from poly-Si for all three dielectric layers after activation anneal and dielectric layers etched off by HF.*

Interestingly, H-effusion from poly-Si after HF-etching off the annealed dielectric layers is independent of the type of hydrogenating layer (see Figure 8). This raised suspicion that there might be interference from HF treatment, which forms a monolayer of hydrogen on poly-Si surface. Thus, H-effusion was measured after first effusion followed by an HF dip (Fig. 9). It was found that the amount of H_2 effused remains the same and is also numerically consistent with a H-monolayer. An alternate protocol (chemical or physical removal of surface H, use of deuterium) needs to be followed to find out the effusion of hydrogen from the *poly*-Si as the hydrogen effused from the monolayer on the surface is dominating in this case.

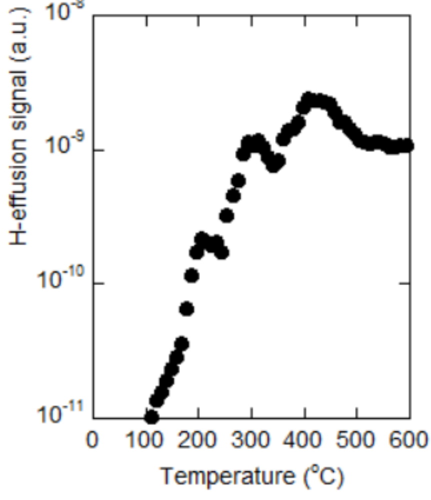

Figure 9. *H-effusion from poly-Si sample after 1st effusion and an HF-dip. A somewhat different shape from Fig. 8 is likely related to higher H-background during this measurement.*

4. Conclusion

In summary, we have explored the passivation mechanism of *poly*-Si/SiO_x passivated contacts under different hydrogenating conditions from different H-containing layers: silicon nitride, alumina, and their stack. The alumina and silicon nitride layers probably release different forms of hydrogen where a lower concentration of hydrogen in Al_2O_3 passivates better than a higher concentration of hydrogen in Si_xN_y. An alternate protocol needs to be developed to find the amount of H jn the *poly*-Si as it cannot be separated from the hydrogen effused from the monolayer of H on the *poly*-Si surface after the HF dip. This understanding could potentially lead to implementation of better process steps to improve V_{oc} and hence, the performance of c-Si cells.

Data availability statement

Data supporting the figures and tables in this article are available from the authors upon request.

Author contributions

Suchismita Mitra-Data Curation, Formal Analysis, Investigation, Methodology, Visualization, Writing – original draft, Dirk Steyn-Investigation, Writing – review & editing, William Nemeth-Data curation, Investigation, Writing – review & editing, Sumit Agarwal-Funding Acquisition, Resources, Writing – review & editing, Paul Stradins- Conceptualization, Funding Acquisition, Methodology, Resources, Supervision, Validation, Visualization, Writing – review & editing

Competing interests

The authors declare that they have no competing interests.

Acknowledgement

This work was authored in part by the National Renewable Energy Laboratory, operated by Alliance for Sustainable Energy, LLC, for the U.S. Department of Energy (DOE) under Contract No. DE-AC36-08GO28308. Funding provided by U.S. Department of Energy Office of Energy Efficiency and Renewable Energy Solar Energy Technologies Office. The views expressed in the article do not necessarily represent the views of the DOE or the U.S. Government. The U.S. Government retains and the publisher, by accepting the article for publication, acknowledges that the U.S. Government retains a nonexclusive, paid-up, irrevocable, worldwide license to publish or reproduce the published form of this work, or allow others to do so, for U.S. Government purposes. Suchismita Mitra would like to thank the Fulbright Commission, the Institute of International Education (IIE) and the United States-India Educational Foundation (USIEF) for awarding the Fulbright Nehru Post-doctoral Fellowship.

References

[1] Hartenstein, M.B., Nemeth, W., Young, D.L., Stradins, P. and Agarwal, S., 2023. Hydrogen Stability and Bonding in SiN_x and Al_2O_3 Dielectric Stacks on Poly-Si/SiO_x Passivating Contacts. ACS Applied Energy Materials, 6(13), pp.7230-7239, https://doi.org/10.1021/acsaem.3c00937.
[2] Kang, D., Sio, H.C., Stuckelberger, J., Liu, R., Yan, D., Zhang, X. and Macdonald, D., 2021. Optimum hydrogen injection in phosphorus-doped polysilicon passivating contacts. ACS Applied Materials & Interfaces, 13(46), pp.55164-55171, https://doi.org/10.1021/acsami.1c17342.
[3] Diggs, A., Crawford, Z., Goga, A., Zhao, Z., Stuckelberger, J. and Zimányi, G.T., 2024. Pinhole Formation by Nucleation-Driven Phase Separation in TOPCon and POLO Solar Cells: Structural Dynamics and Optimization. ACS Applied Energy Materials, 7(8), pp.3414-3423, https://doi.org/10.1021/acsaem.4c00171.
[4] Jafari, S., Varshney, U., Hoex, B., Meyer, S. and Lausch, D., 2021. Understanding light- and elevated temperature-induced degradation in silicon wafers using hydrogen effusion mass spectroscopy. IEEE Journal of Photovoltaics, 11(6), pp.1363-1369, https://doi.org/10.1109/JPHOTOV.2021.3104194.
[5] Cartier, E., Stathis, J.H. and Buchanan, D.A., 1993. Passivation and depassivation of silicon dangling bonds at the Si/SiO2 interface by atomic hydrogen. Applied Physics Letters, 63(11), pp.1510-1512, https://doi.org/10.1063/1.110758.
[6] Truong, T.N., Yan, D., Chen, W., Tebyetekerwa, M., Young, M., Al-Jassim, M., Cuevas, A., Macdonald, D. and Nguyen, H.T., 2020. Hydrogenation mechanisms of poly-Si/SiO_x passivating contacts by different capping layers. Solar RRL, 4(3), p.1900476, https://doi.org/10.1002/solr.201900476.